Journal of the Korean Chemical Society
2023, *Vol. 67, No. 5*
Printed in the Republic of Korea
https://doi.org/10.5012/jkcs.2023.67.5.348

Crystal Structure of p97-N/D1 Hexamer Complexed with FAF1 UBX Domain

Wonchull Kang[†,‡,*]

[†]*Department of Chemistry and Integrative Institute of Basic Science, College of Natural Sciences, Soongsil University, Seoul 06978, Korea*
[‡]*Department of Green Chemistry and Materials Engineering, Soongsil University, Seoul 06978, Korea*
**E-mail: wonchullkang@ssu.ac.kr*
(Received August 21, 2023; Accepted September 3, 2023)

ABSTRACT. p97, a universally conserved AAA+ ATPase, holds a central position in the ubiquitin-proteasome system, orchestrating myriad cellular activities with significant therapeutic implications. This protein primarily interacts with a diverse set of adaptor proteins through its N-terminal domain (NTD), which is structurally located at the periphery of the D1 hexamer ring. While there have been numerous structural elucidations of p97 complexed with adaptor proteins, the stoichiometry has remained elusive. In this work, we present the crystal structure of the p97-N/D1 hexamer bound to the FAF1-UBX domain at a resolution of 3.1 Å. Our findings reveal a 6:6 stoichiometry between the p97 hexamer and FAF1-UBX domain, deepening our understanding from preceding structural studies related to p97-NTD and UBX domain-containing proteins. These insights lay the groundwork for potential therapeutic interventions addressing cancer and neurodegenerative diseases.

Key words: p97, valosin-containing protein, Fas-associated factor 1, Ubiquitin regulatory X, UBX

INTRODUCTION

p97, a highly conserved AAA+ adenosine triphosphatase (ATPase), holds a pivotal role within the ubiquitin-proteasome system (UPS). In *Saccharomyces cerevisiae*, its counterpart is referred to as Cdc48. It is chiefly involved in the extraction and disassembly of substrates across diverse cellular sites, influencing an array of cellular processes from proteasomal and lysosomal degradation to membrane fusion, cell cycle control, the regulation of apoptosis, and DNA damage repair.[1]

Structurally, p97 assembles as a homohexamer. Each monomer is composed of three domains: two ATPase domains (D1 and D2), an N-terminal domain (NTD), and a disordered C-terminal tail domain (CTD). The D1 and D2 domains form two parallel hexameric rings, with the NTD located at the periphery of the D1 ring.[2]

Numerous adaptor proteins, each outfitted with ubiquitin-binding sites, directly interface with the p97-NTD. This association expedites the identification of ubiquitylated target proteins within the UPS.[3]

Such adaptor proteins serve as structural scaffolds, presenting additional interaction sites, orchestrating the p97 complex assembly, and correctly aligning substrate for ensuing operations.[4] Among the notable cofactors are Ufd1-Npl4 and p47.[3a,5] Many of these adaptor proteins, including p47 and Fas-associated factor 1 (FAF1), feature the ubiquitin regulatory X (UBX) domain.[6]

FAF1 is identified as a Fas-interacting protein and impedes proteasomal protein degradation, either through its alliance with p97 or with ubiquitinated substrates.[7] It possesses a multifaceted structure with domains like ubiquitin-associating (UBA) domain, two tandem ubiquitin-like (UBL) domains, a UAS domain, a coiled-coil domain, and a UBX domain (*Fig.* 1).[4,8]

The UBA domain interacts with ubiquitins on the substrates, and the UBX domain engages with the p97-NTD.[8]

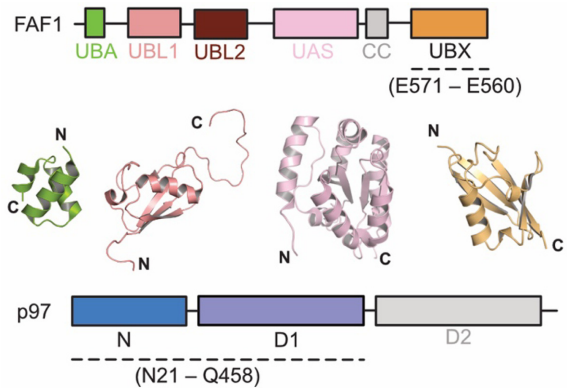

***Figure* 1.** Schematic representations of the domains in FAF1 and p97. Dashed lines indicate the regions examined in this crystallographic study. The structures of the domains in FAF1 were retrieved from the RCSB Protein Data Bank: UBA (PDB ID: 3E21), UBL1 (PDB ID: 2DZM), UAS (PDB ID: 2EC4), and UBX (PDB ID: 3QCA).

Via these interactions, FAF1 facilitates the degradation of endoplasmic reticulum degradation (ERAD) substrates by binding Lys-48- and Lys-63-linked polyubiquitylated substrates through its UBA domain.[9]

In another key interaction, FAF1 interacts with p65 subunit of nuclear factor kappa-light-chain-enhancer of activated B cells (NF-κB) , inhibiting its nuclear translocation and subsequent gene activation.[10] Typically, the NF-κB heterodimer is sequestered in the cytoplasm by Iκ-Bα.[11] However, upon phosphorylation and ubiquitylation of Iκ-Bα, it undergoes UPS-mediated degradation.[11] Owing to these multifaceted roles, both the p97-FAF1 complex and FAF1 in isolation emerge as attractive therapeutic candidates in the combat against cancer and neurodegenerative diseases.[12]

The stoichiometry of the p97 complex, especially in relation to its adaptor proteins, remains an area of ambiguity. Cryogenic electron microscopy (cryo-EM) has elucidated that the Ufd1-Npl4 and p97 hexamer forms a complex with a 1:6 stoichiometry.[3a,5b] Furthermore, biophysical studies have revealed that monomeric p47 binds to the p97 hexamer, reflecting a 1:6 stoichiometry.[13] Structural analyses into the FAF1-p97 complex have shown a 3:6 stoichiometry.[14]

In this study, we determined the crystal structure of the p97-N/D1 hexamer complexed with the FAF1-UBX domain, achieving a resolution of 3.1 Å. Our structural dissection provides compelling insights into the stoichiometry linking the p97 hexamer and the UBX domain. Prior crystallographic studies have disclosed a 1:1 binding affinity between the p97-NTD and the UBX domain.[15] Our findings augment this narrative, shedding light on the interactions of the pseudo full-length p97-N/D1 hexamer with UBX domain-containing proteins.

EXPERIMENTAL

Crystallization and X-ray Data Collection

The human p97-N/D1 domain (residues 21-458) and the human FAF1 UBX domain (residues 575-650) were expressed and purified separately as previously described.[16] The purified FAF1 UBX domain was trimmed at the N-terminus, starting at Glu575 instead of Glu571, which differs from the previous study.[16] The purified p97-N/D1 and FAF1 UBX were mixed at the same molar ratio for crystallization. Crystallization conditions were initially screened using commercial screening kits from Hampton Research, and Qiagen. Under optimized condition, a drop consisting of 2 μL protein solution was mixed with an equal volume of reservoir solution. The reservoir solution was composed of 0.2 M sodium acetate, 0.1 M sodium citrate (pH 5.6), and 5% polyethylene glycol 4000. The mixture was then equilibrated against 0.5 mL reservoir solution at 295 K. Crystals were briefly soaked in a cryoprotective solution made of the reservoir solution with an additional 25% (v/v) glycerol and were directly flash-cooled in liquid nitrogen prior to data collection. The diffraction data were collected at the beamline BL17A in the Photon Factory Advanced Ring (PF-AR, Tsukuba, Japan) using the CCD detector Quantum 210R (ADSC). The data were processed with XDS and scaled with AIMLESS in the Collaborative Computational Project Number 4 (CCP4) suite.[17] Data collection statistics are summarized in *Table* 1.

***Table* 1.** Crystallographic statistics for data collection and refinement

PDB ID	8KG2
Data Collection	
Wavelength (Å)	1.0000 Å
Space group	*P* 1
Total reflections	582,011 (29,498)
Unique reflections	150,419 (7,521)
Cell dimensions	
a, *b*, *c* (Å)	106.6, 134.4, 148.2
α, β, γ (°)	71.5, 80.8, 87.5
Resolution (Å)	48.80–3.10 (3.15–3.10)
R_{meas}	0.088 (0.839)
$CC_{1/2}$	0.998 (0.704)
$I/\sigma I$	7.7 (1.2)
Completeness (%)	97.4 (97.8)
Multiplicity	3.9 (3.9)
Refinement	
Resolution (Å)	48.80–3.10
R_{work} / R_{free} [a]	0.197 / 0.246
No. atoms	
Protein	48,411
Ligand	324
B-factors	
Overall	91
Protein	91
Ligand	66
R.m.s. deviations	
Bond lengths (Å)	0.006
Bond angles (°)	1.560
Ramachandran plot (%)	
Favored	95.3
Allowed	3.2
Outliers	1.4

Values in parentheses refer to the highest resolution shell.
[a]$R_{work} = \Sigma||F_{obs}| - |F_{calc}||/\Sigma|F_{obs}|$, where R_{free} was calculated for a randomly chosen 5% of reflections that were not used for structure refinement, and R_{work} was calculated for the remaining reflections.

Structure Determination and Refinement

Initial phases were determined by the Phaser in the PHENIX suite and using the p97-N/D1 hexamer as a search model (PDB ID: 5DYG).[18] The model of the FAF1 UBX domain was manually built, with reference to the crystal structure of p97-N in complex with FAF1 UBX domain (PDB ID: 3QC8).[15b] Structure refinement was carried out using phenix.refine in the PHENIX suite, and manual refinement was subsequently performed interatively using COOT.[19] Omit maps was calculated using Polder Maps in the PHENIX suite.[19b] Figures were prepared using the PyMOL (PyMOL Molecular Graphics System, Version 2.5.0 Schrödinger, LLC). Coordinates and structure factors have been deposited in the Protein Data Bank under accession code 8KG2 and are publicly available as of the date of publication.

RESULTS AND DISCUSSION

Overall Structure

Previously, we reported the crystal structure of p97-NTD complexed with FAF1-UBX, uncovering the atomic details of the binding interface.[15b] Following this, we examined the structure of the p97-N/D1 hexamer complexed with FAF-UBX to determine if the 1:1 stoichiometry observed in the p97-NTD remains consistent in the p97-N/D1 hexamer. In contrast, cryo-EM and biophysical studies have indicated a 3:6 stoichiometry for the full length FAF1 and p97, suggesting that three FAF1 units bind to the p97 hexamer. Given that the UBX domain is the sole binding motif for p97, the binding stoichiometry is intriguing. While our initial crystallization attempts of the p97-N/D1 hexamer with the FAF1 UBX domain did not yield high-quality crystals, a triple mutant (E192A, D193A, and E194A) of p97-N/D1-developed using the surface-entropy reduction method-successfully produced them. Additionally, the N-terminus of the FAF1 UBX domain was truncated to avoid disrupting the crystal lattice interaction, based on a previous crystallographic study.[16] Consequently, we determined the crystal structure of the p97-N/D1 hexamer complexed with the FAF1 UBX domain at a resolution of 3.1 Å, refining it to R_{work} values of 19.7% and R_{free} of 24.6% (*Table* 1).

Within the asymmetric unit of the triclinic crystal system, we identified two p97-N/D1 hexamers and twelve FAF1 UBX domains. Composite omit maps for the FAF1 UBX domain corroborated the accuracy of our model (*Fig*. 2a), and the $2F_o$-F_c electron density maps for FAF1 UBX domain further validated the presence of the UBX domains upon reaching refinement convergence (*Fig*. 2b).

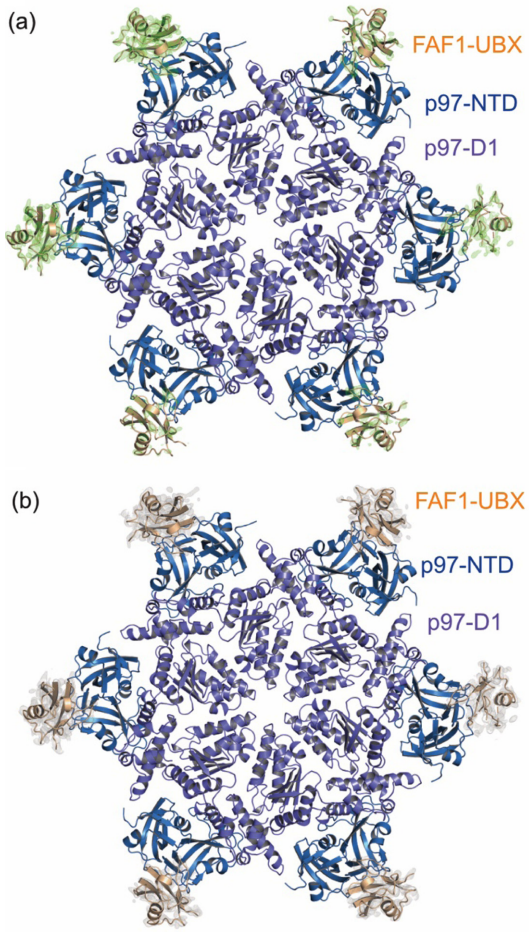

***Figure* 2.** Overall structure of the p97 in complexed with the FAF1-UBX domain. Ribbon diagrams are overlaid with (a) omit F_o-F_c electron density maps contoured at 3.0 times RMSD (shown in green) and (b) $2F_o$-F_c electron density maps contoured at 1.0 times RMSD (shown in gray). The omit F_o-F_c electron density maps were generated using Polder Maps from the PHENIX suite.

Interestingly, the crystal structure of p97-N/D1 complexed with the p47 UBX domain showed that three UBX domains bind to the p97-N/D1 hexamer due to an additional binding motif preceding the UBX domain, known as the SHP box.[15a] Therefore, our current structure suggests that the FAF1 UBX domain binds to the p97 N/D1 hexamer in a 6:6 stoichiometry.

Comparative Analysis of p97-FAF1 Complex

To construct a comprehensive model of the p97-FAF1 complex, we manually superimposed our crystal structure onto cryo-EM envelopes. Although rigid-body fitting attempts using ChimeraX or the PHENIX suite were unsuccessful with the full-length p97 model,[19b,20] our p97-N/D1 structure was manually fitted into the central position manually

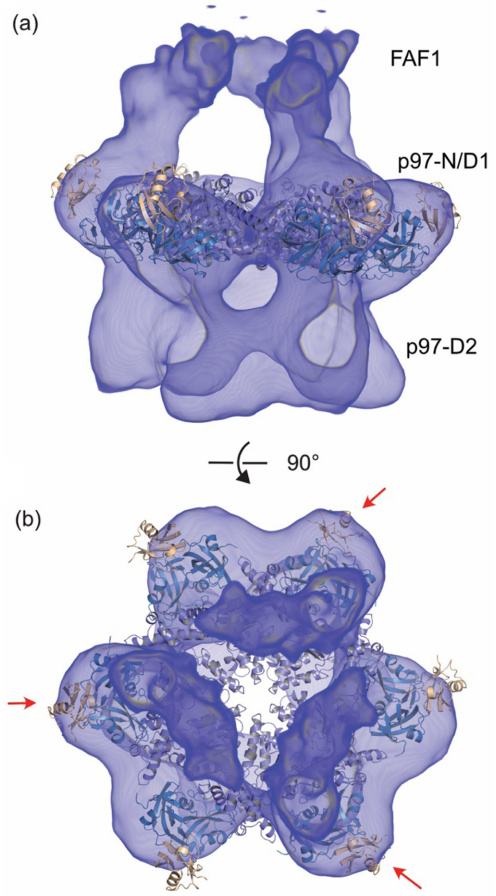

***Figure* 3.** Overlay of the crystal structure onto the cryo-EM envelopes of the p97-FAF1 complex (EMDB accession code EMD-2319). The crystal structure of the p97-N/D1 hexamer in complex with the FAF1-UBX domain was manually aligned to the cryo-EM envelopes. Shown are the side view (a) and top view (b) of the complex. The red arrow indicates the UBX domain, which fits well into the cryo-EM envelopes.

within the envelopes. Intriguingly, upon this fitting, three of the UBX domains were predominantly situated within the envelopes (*Fig*. 3). In contrast, the remaining UBX domains were located outside these envelopes, which signifies a stoichiometry of 3:6. An interesting observation was the presence of N-terminal blobs that showcased a pseudo 3-fold symmetrical density situated above the UBX domain. This was intricately connected to the N-terminus via narrow envelopes. Since the UBX domain in FAF1 is the sole binding motif, the remaining domains in FAF1, comprising 570 amino acid residues, are depicted as 3-fold symmetrical density in the cryo-EM envelopes. The envelope containing the N-terminal domains, including UBA, UBL, UAS, and CC, in FAF1 spans across two p97 protomers. Given the hypothesis that six full-length FAF1 units bind to p97, the N-terminal blob could potentially obstruct the binding of the adjacent protomer. However, further structural studies are required to resolve the details. Thus, based on our structure and structural alignments, UBX domain alone obviously binds to the p97 hexamer in a 6:6 stoichiometry, because the long N-terminal domains of FAF1 are not disturb spatially.

CONCLUSION

In this study, we elucidated the crystal structure of p97-N/D1 hexamer in complex with FAF1 UBX domain, revealing a 6:6 stoichiometry. Combined with previous cryo-EM data, our results could suggest that the three full-length FAF1 interacts with full-length p97 hexamer at a 3:6 ratio. The distinctive arrangement of the UBX domains within the cryo-EM envelopes supports this stoichiometry. Additionally, potential steric hindrance from the N-terminal domains of FAF1 is anticipated at a 6:6 ratio. However, additional structural studies are required to achieve high-resolution model. These insights not only deepen our understanding of the p97-FAF1 interaction but also pave the way for further research into its functional roles and potential therapeutic applications.

Acknowledgments. This research was supported by the Basic Science Research Program of the National Research Foundation of Korea (NRF) (2021R1A6A1A10044154 and 2022R1C1C1004221 to W.K.). We thank the staff at the Beamline 17A of the Photon Factory Advanced Ring in Japan.

REFERENCES

1. (a) Xia, D.; Tang, W. K.; Ye, Y., *Gene.* **2016**, *583*, 64; (b) Meyer, H.; Weihl, C. C., *J. Cell. Sci.* **2014**, *127*, 3877; (c) Erzberger, J. P.; Berger, J. M., *Annu Rev Biophys Biomol. Struct.* **2006**, *35*, 93.
2. (a) DeLaBarre, B.; Brunger, A. T., *Nat. Struct. Biol.* **2003**, *10*, 856; (b) Banerjee, S.; Bartesaghi, A.; Merk, A.; Rao, P.; Bulfer, S. L.; Yan, Y.; Green, N.; Mroczkowski, B.; Neitz, R. J.; Wipf, P.; Falconieri, V.; Deshaies, R. J.; Milne, J. L.; Huryn, D.; Arkin, M.; Subramaniam, S., *Science* **2016**, *351*, 871.
3. (a) Meyer, H.; Bug, M.; Bremer, S., *Nat. Cell. Biol.* **2012**, *14*, 117; (b) DeLaBarre, B.; Brunger, A. T., *Nature Structural Biology* **2003**, *10*, 856.
4. Kloppsteck, P.; Ewens, C. A.; Forster, A.; Zhang, X.; Freemont, P. S., *Biochim Biophys Acta* **2012**, *1823*, 125.
5. (a) Kondo, H.; Rabouille, C.; Newman, R.; Levine, T. P.; Pappin, D.; Freemont, P.; Warren, G., *Nature* **1997**, *388*, 75; (b) Pye, V. E.; Beuron, F.; Keetch, C. A.; McKeown, C.; Robinson, C. V.; Meyer, H. H.; Zhang, X.; Freemont, P.

S., *Proc. Natl. Acad. Sci. U.S.A.* **2007**, *104*, 467.
6. Schuberth, C.; Buchberger, A., *Cell. Mol. Life. Sci.* **2008**, *65*, 2360.
7. (a) Ryu, S. W.; Chae, S. K.; Lee, K. J.; Kim, E., *Biochemical and Biophysical Research Communications* **1999**, *262*, 388; (b) Chu, K.; Niu, X.; Williams, L. T., *Proceedings of the National Academy of Sciences of the United States of America* **1995**, *92*, 11894.
8. Song, E. J.; Yim, S. H.; Kim, E.; Kim, N. S.; Lee, K. J., *Molecular and Cellular Biology* **2005**, *25*, 2511.
9. (a) Kim, H. J.; Song, E. J.; Lee, Y. S.; Kim, E.; Lee, K. J., *J. Biol. Chem.* **2005**, *280*, 8125; (b) Song, J.; Park, J. K.; Lee, J. J.; Choi, Y. S.; Ryu, K. S.; Kim, J. H.; Kim, E.; Lee, K. J.; Jeon, Y. H.; Kim, E. E., *Protein Sci.* **2009**, *18*, 2265.
10. Park, M. Y.; Jang, H. D.; Lee, S. Y.; Lee, K. J.; Kim, E., *Journal of Biological Chemistry* **2004**, *279*, 2544.
11. Novack, D. V., *Cell. Res.* **2011**, *21*, 169.
12. Menges, C. W.; Altomare, D. A.; Testa, J. R., *Cell. Cycle.* **2009**, *8*, 2528.
13. Conicella, A. E.; Huang, R.; Ripstein, Z. A.; Nguyen, A.; Wang, E.; Lohr, T.; Schuck, P.; Vendruscolo, M.; Rubinstein, J. L.; Kay, L. E., *Proc. Natl. Acad. Sci. U.S.A.* **2020**, *117*, 26226.
14. Ewens, C. A.; Panico, S.; Kloppsteck, P.; McKeown, C.; Ebong, I. O.; Robinson, C.; Zhang, X.; Freemont, P. S., *J. Biol. Chem.* **2014**, *289*, 12077.
15. (a) Dreveny, I.; Kondo, H.; Uchiyama, K.; Shaw, A.; Zhang, X.; Freemont, P. S., *EMBO Journal* **2004**, *23*, 1030; (b) Kim, K. H.; Kang, W.; Suh, S. W.; Yang, J. K., *Proteins* **2011**, *79*, 2583; (c) Kim, S. J.; Cho, J.; Song, E. J.; Kim, S. J.; Kim, H. M.; Lee, K. E.; Suh, S. W.; Kim, E. E., *J. Biol. Chem.* **2014**, *289*, 12264; (d) Arumughan, A.; Roske, Y.; Barth, C.; Forero, L. L.; Bravo-Rodriguez, K.; Redel, A.; Kostova, S.; McShane, E.; Opitz, R.; Faelber, K.; Rau, K.; Mielke, T.; Daumke, O.; Selbach, M.; Sanchez-Garcia, E.; Rocks, O.; Panakova, D.; Heinemann, U.; Wanker, E. E., *Nat. Commun.* **2016**, *7*, 13047; (e) Banchenko, S.; Arumughan, A.; Petrovic, S.; Schwefel, D.; Wanker, E. E.; Roske, Y.; Heinemann, U., *Structure* **2019**, *27*, 1830.
16. Kang, W.; Yang, J. K., *Acta Crystallogr Sect F Struct Biol Cryst Commun* **2011**, *67*, 1199.
17. (a) Winn, M. D.; Ballard, C. C.; Cowtan, K. D.; Dodson, E. J.; Emsley, P.; Evans, P. R.; Keegan, R. M.; Krissinel, E. B.; Leslie, A. G.; McCoy, A.; McNicholas, S. J.; Murshudov, G. N.; Pannu, N. S.; Potterton, E. A.; Powell, H. R.; Read, R. J.; Vagin, A.; Wilson, K. S., *Acta Crystallogr D Biol Crystallogr* **2011**, *67*, 235; (b) Kabsch, W., Xds. *Acta Crystallogr D Biol Crystallogr* **2010**, *66*, 125.
18. Tang, W. K.; Xia, D., *Sci. Rep.* **2016**, *6*, 20037.
19. (a) Emsley, P.; Lohkamp, B.; Scott, W. G.; Cowtan, K., *Acta Crystallogr D Biol Crystallogr* **2010**, *66*, 486; (b) Adams, P. D.; Afonine, P. V.; Bunkoczi, G.; Chen, V. B.; Davis, I. W.; Echols, N.; Headd, J. J.; Hung, L. W.; Kapral, G. J.; Grosse-Kunstleve, R. W.; McCoy, A. J.; Moriarty, N. W.; Oeffner, R.; Read, R. J.; Richardson, D. C.; Richardson, J. S.; Terwilliger, T. C.; Zwart, P. H., *Acta Crystallogr D Biol Crystallogr* **2010**, *66*, 213.
20. Pettersen, E. F.; Goddard, T. D.; Huang, C. C.; Meng, E. C.; Couch, G. S.; Croll, T. I.; Morris, J. H.; Ferrin, T. E., *Protein Sci.* **2021**, *30*, 70.